

Colour-producing β -keratin nanofibres in blue penguin (*Eudyptula minor*) feathers

Liliana D'Alba¹, Vinodkumar Saranathan^{2,*†},
Julia A. Clarke³, Jakob A. Vinther⁴,
Richard O. Prum² and Matthew D. Shawkey^{1,*†}

¹Department of Biology and Integrated Bioscience Program,
University of Akron, Akron, OH 44325-3908, USA

²Department of Ecology and Evolutionary Biology and Peabody Museum
of Natural History, Yale University, New Haven, CT 06520, USA

³Department of Geological Sciences, University of Texas at Austin,
1 University Station C1100, Austin, TX 78712, USA

⁴Department of Geology and Geophysics, Yale University, New Haven,
CT 06520, USA

*Authors for correspondence (shawkey@uakron.edu;
vinodkumar.saranathan@yale.edu).

†These authors contributed equally to the study.

The colours of living organisms are produced by the differential absorption of light by pigments (e.g. carotenoids, melanins) and/or by the physical interactions of light with biological nanostructures, referred to as structural colours. Only two fundamental morphologies of non-iridescent nanostructures are known in feathers, and recent work has proposed that they self-assemble by intracellular phase separation processes. Here, we report a new biophotonic nanostructure in the non-iridescent blue feather barbs of blue penguins (*Eudyptula minor*) composed of parallel β -keratin nanofibres organized into densely packed bundles. Synchrotron small angle X-ray scattering and two-dimensional Fourier analysis of electron micrographs of the barb nanostructure revealed short-range order in the organization of fibres at the appropriate size scale needed to produce the observed colour by coherent scattering. These two-dimensional quasi-ordered penguin nanostructures are convergent with similar arrays of parallel collagen fibres in avian and mammalian skin, but constitute a novel morphology for feathers. The identification of a new class of β -keratin nanostructures adds significantly to the known mechanisms of colour production in birds and suggests additional complexity in their self-assembly.

Keywords: structural colour; nanofibres;
biophotonics

1. INTRODUCTION

Colour-producing biological nanostructures have diverse morphologies that may be periodic in one, two or three dimensions, with either long-range crystal-like periodicity or merely short-range order at nearest neighbour length scales (i.e. quasi-ordered) [1,2]. In bird feathers, one- or two-dimensional

organized arrays of melanosomes and β -keratin in feather barbules create iridescent colours (e.g. peacocks and hummingbirds), while three-dimensional quasi-ordered arrays of β -keratin and air in the spongy medullary layer of the barb rami produce non-iridescent colours (e.g. Eastern Bluebird *Sialia sialis*) [2]. For over four decades, only two fundamental morphologies of spongy medullary structural colour-producing nanostructures have been recognized [1,2]. The first is a quasi-periodic array of spherical air bubbles in a β -keratin matrix and the second is a tortuous network of air and β -keratin channels of similar widths and shapes. However, these nanostructures have been examined using electron microscopy (EM) in only a limited number of bird species [2]. Broader sampling is needed to elucidate the evolutionary history of barb structural colours and identify novel biophotonic nanostructures.

Many species in at least four penguin genera (Aves, Spheniscidae: *Eudyptes*, *Eudyptula*, *Pygoscelis* and *Aptenodytes*) exhibit prominent to marginal, non-iridescent blue coloration in the contour feathers of the dorsum and wing coverts, but the mechanism of this colour production is currently unexplored. Here, we investigate the mechanistic basis of the blue coloration in blue penguins (*Eudyptula minor*) from New Zealand.

2. MATERIAL AND METHODS

We use synchrotron small angle X-ray scattering (SAXS), light and EM, normal-incidence spectrophotometry and refractive index matching to characterize the nanostructure and colour production of blue feather barbs of blue penguins. To examine the relationship between nanostructure and optical function, we compare the measured optical reflectance with colour prediction from SAXS data collected from intact feather barbs using standard protocol [3] and two-dimensional Fourier analysis [2] of transmission EM (TEM) images of the blue barb nanostructure. For detailed methods, see the electronic supplementary material.

3. RESULTS

The blue colour in the blue penguin dorsal plumage and wing coverts is largely restricted to the distalmost barbs at the tips of feather vanes (figure 1b,c), which together form the exposed surface of the densely packed plumage. The blue barbs are vertically flattened and either lack or have severely reduced barbules (figure 1c). The blue barbs have three discrete layers arranged as follows from the obverse (outer) to reverse (inner) surface within the barb ramus: a 1–5 μm outer cortex of unstructured β -keratin above a 20 μm layer of medullary cells containing densely packed bundles of parallel β -keratin fibres surrounded by air spaces, overlying a basal layer of cortical cells containing solid β -keratin with discrete aggregations of large ellipsoidal melanosomes [4] surrounded by keratin (figure 1d,e). The fibres average 183.8 ± 4.0 (\pm s.e., $n = 50$) nm in diameter (figure 1e) and are between 3 and 14 μm in length. Based on the presence of keratinized cell boundaries surrounding them, the dense bundles of fibres are inside the medullary cells of the barb (electronic supplementary material, figure S1a,b). Neighbouring fibres within a bundle are parallel to the surface of the cell and predominantly organized along the longitudinal axis of the barb ramus, although this direction is somewhat variable

Electronic supplementary material is available at <http://dx.doi.org/10.1098/rsbl.2010.1163> or via <http://rsbl.royalsocietypublishing.org>.

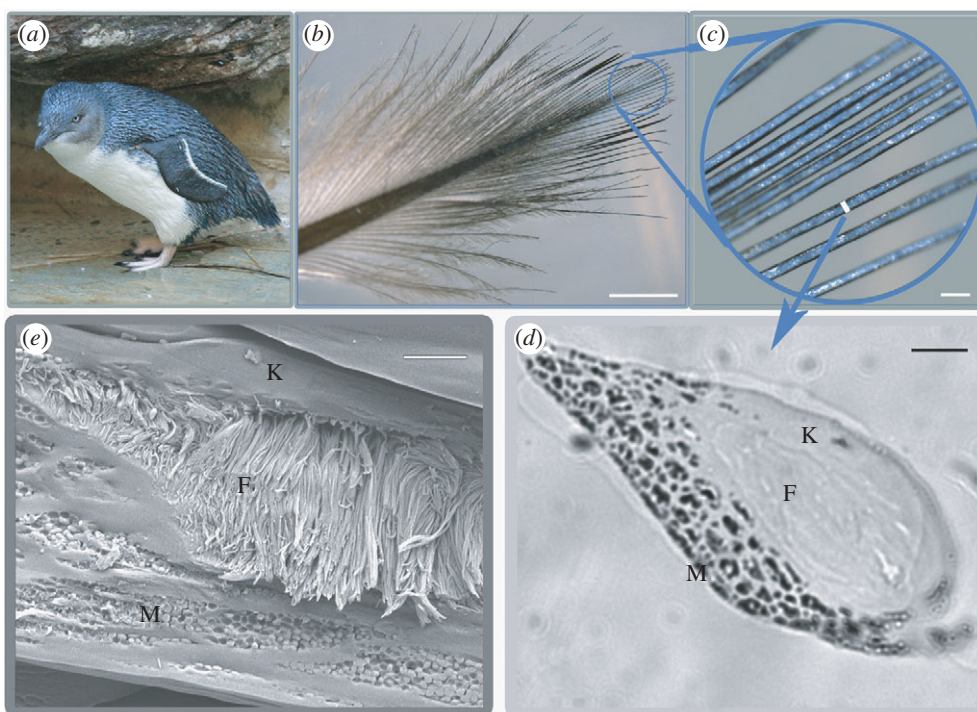


Figure 1. Morphology of *E. minor* feather barbs. (a) Blue penguin. Photo credit: John Denman, Australia (by permission). (b) Photograph of a contour feather, with distal blue area circled. (c) Close-up of blue barbs. (d) Light microscope image of a lateral section of blue barbs showing the outer cortex (K), medullary keratin nanofibres (F), and basal melanosomes (M). (e) Scanning electron micrograph image of a cross section of a blue barb. Scale bars, (b) 3 mm, (c) 200 μm (d) 10 μm , (e) 2 μm .

among cells (electronic supplementary material, figure S1a–c). In some cases, the ends of fibre bundles wrap around spirally within a cell to end up perpendicular to the original orientation (electronic supplementary material, figure S1c). The spaces between the β -keratin fibres are filled with air (figure 1e and electronic supplementary material, figure S1) as in other spongy medullary barb nanostructures [2].

Infiltration of the medullary air spaces with a fluid matching the refractive index of β -keratin demonstrated that the blue colour is structural in origin (see the electronic supplementary material). Upon infiltration, the blue barbs turned black (electronic supplementary material, figure S2) because light scattering is reduced by the matching refractive index between the fibres and the fluid-filled surrounding spaces [2].

The two-dimensional SAXS pattern from blue penguin barbs (figure 2a) is bow tie-shaped, consistent with scattering from an amorphous, or quasi-ordered packing of parallel cylindrical fibres [5]. It exhibits an arc-like broadening in the azimuthal direction, indicating that the majority of the fibres are oriented along the long axis of the barb rami, with some additional variation in the curvature of the fibre bundles within each cell (figure 1e and electronic supplementary material, figure S1). At small spatial length scales ($q > 0.07 \text{ nm}^{-1}$), the azimuthally integrated SAXS profile (figure 2b) of the blue penguin barb nanostructures follows Porod's Law or the null expectation for lack of structuring. However, at intermediate length scales ($0.02 < q < 0.05 \text{ nm}^{-1}$) relevant for visible structural colour production, the SAXS profile exhibits a broad structural correlation peak owing to the close-packed nature of the nanofibres at a peak spatial frequency of

0.03476 nm^{-1} and two weak higher order peaks (figure 2b). The widening of the principal scattering peak is caused by polydispersity, or variation in the nanofibre radii, and by the lack of long-range order. The position of the primary peak, q_0 , gives the spatial correlation length or the distance between neighbouring fibre centres, $d = 2\pi/q_0$, while the full width at half-maximum, Δq , of the peak is a measure of the range of spatial quasi-periodic order, or coherence length, $\xi = 2\pi/\Delta q$, within the system. The SAXS data provide a value of 181 nm for d , confirming the presence of a dominant length scale of structural periodicity that is on the order of visible wavelengths of light and highly congruent with the measurements of the nanofibre dimensions from electron micrographs. However, ξ is only 290 nm (approx. 1.6 d), which is lower than the range reported for three-dimensional quasi-ordered photonic nanostructures found in feather barbs ($\xi \sim 3\text{--}5d$) [3], suggesting that the two-dimensional penguin nanofibre nanostructures have more variation in the nearest neighbour spacing or less order when compared with three-dimensional barb nanostructures. The higher order SAXS peaks at 0.06298 and 0.10517 nm^{-1} conform quite well to the theoretical cylindrical form factor, or the simulated scattering peaks calculated from single fibres of mean radius 80 nm and length 3 μm with a 15 per cent variation in radii (figure 2b, see the electronic supplementary material).

By contrast, azimuthal averages from brown and white feather barbs of *E. minor* show good agreement with Porod's Law at all q , indicating the absence of any medullary nanostructure (figure 2b). The blue colour is thus restricted to those barbs that have fibrillar nanostructures.

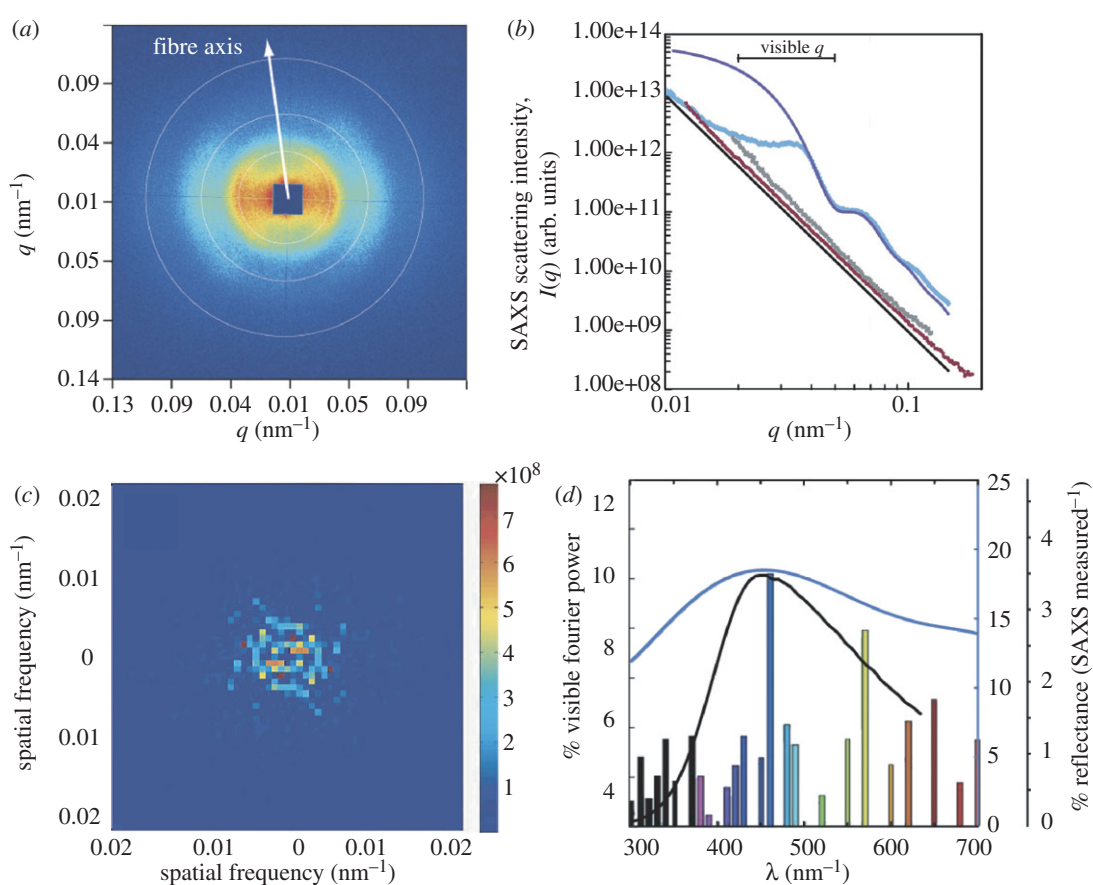


Figure 2. Structural and optical analyses of penguin barb nanostructures using SAXS and two-dimensional Fourier analysis of TEMs. (a) Representative two-dimensional SAXS pattern (unmasked) from a blue barb of *E. minor*. The false colour scale corresponds to the logarithm of scattering intensity. The concentric white circles denote the location of scattering peaks. The orientation axis of the fibre bundles corresponding to the observed SAXS pattern is indicated. (b) Azimuthally averaged scattering profiles (scattering wavevector q versus intensity $I(q)$) calculated from SAXS patterns of blue (light blue line), brown (brown line) and white (grey line) *E. minor* barbs plotted on a log–log scale. The simulated scattering form factor (dark blue line) of a single cylindrical nanofibre of length 3 μm , with an 80 nm radius and 15% polydispersity in radii is shown for comparison (in arbitrary units). The Porod asymptote (black line) indicates the null expectation for asymptotic scattering from an unstructured material. The excellent congruence of the SAXS profiles of white and brown penguin barbs to the Porod asymptote indicates that, unlike blue barbs, they are not nanostructured. (c) Two-dimensional Fourier power spectrum of a TEM cross section of a blue barb of *E. minor*. (d) Measured reflectance spectra (blue line and ordinates), SAXS reflectance predictions (black line and ordinates) and Fourier-predicted reflection spectrum (coloured bars approximating human-perceived colours at these wavelengths).

The prediction of the optical reflectance spectra based on the SAXS correlation peak agrees well using an average refractive index (n_{av}) value of 1.24, which corresponds to a keratin volume fraction of 0.41 [6] (figure 2d). The broader width of the measured reflectance peak when compared with the single-scattering SAXS prediction is probably owing to multiple scattering of light, which interacts strongly with the inherent disorder of the nanostructure [3].

The two-dimensional Fourier power spectra of TEM cross sections (electronic supplementary material, figure S1b,c) of the penguin barb quasi-ordered nanostructure were ring-like (figure 2c), further corroborating the presence of a characteristic peak length scale at the spatial periodicity of the interfibre distances, and the lack of long-range order. The predicted hue (458 nm) obtained from Fourier analyses [7] reasonably matched the measured hue of 447 nm (figure 2d). Using the pixel contrast of the dark and light pixels in TEM images (e.g. electronic supplementary material, figure S1b,c), we estimated n_{av} to be

1.29 ± 0.05 (\pm s.e., $n = 10$ images) which is close to the SAXS estimate.

4. DISCUSSION

The blue penguin feathers characterized here represent the first reported case of a non-iridescent structural colour based on two-dimensional quasi-ordered arrays of parallel β -keratin nanofibres [2]. Both SAXS data and Fourier analysis of TEM sections demonstrate structuring at the appropriate size scale to produce the observed colour by coherent light scattering. The penguin nanostructure is evolutionarily convergent with the two-dimensional quasi-ordered arrays of parallel collagen fibres found in non-iridescent, structurally coloured skin of birds and mammals [2,8]. Both nanostructures have evolved independently in distantly related lineages, probably as a result of selection to produce non-iridescent structural hues, despite anatomical and material differences.

It has been hypothesized that the channel- and sphere-type barb nanostructures are self-assembled by phase separation through either spinodal decomposition or nucleation-and-growth, respectively [3,9]. β -keratin is a filament-forming molecular polymer [10] and other polymers are known to produce a wide variety of nanoscale, macromolecular structures under different physical conditions [11]. Specifically, phase transitions between disordered parallel cylinder phases to nucleation-and-growth and spinodal morphologies are well documented in soft-matter systems like block copolymer melts [12]. We therefore hypothesize that the penguin nanofibres are self-assembled by polymerization of intracellular β -keratin, perhaps through hierarchical assembly from smaller β -keratin fibrils.

Our results suggest that the blue penguin has probably evolved to exploit β -keratin's inherent capacity for intracellular, hierarchical fibre self-assembly to produce photonic nanostructures [9,10]. Both nanofibres and photonic structures have diverse applications ranging from biomedicine to electronics. Identifying self-assembly processes in nature may provide key insights that could be applied to inexpensive production of synthetic analogues. Thus, characterization of these novel β -keratin nanofibres not only adds considerably to the known mechanisms of colour production in birds but also expands our understanding of biophotonic colours, and may provide biomimetic inspiration for the next generation of self-assembled, multi-functional meta-materials.

This work was carried out under the guidelines of the University of Akron and the US fish and wildlife Service.

This work was supported by U. Akron start-up funds and AFOSR grant FA9550-09-1-0159 (both to M.D.S.) and Yale University funds (V.S.) and an NSF (DBI) grant (R.O.P.). SAXS data were collected at beam line 8-ID-I at the Advanced Photon Source at Argonne National Laboratories with the help of Dr Alec Sandy and Dr Suresh Narayanan, and supported by the US Department of Energy, Office of Science, Office of Basic Energy Sciences, under contract no. DE-AC02-06CH11357.

- 1 Srinivasarao, M. 1999 Nano-optics in the biological world: beetles, butterflies, birds, and moths. *Chem. Rev.* **99**, 1935–1961. ([doi:10.1021/cr970080y](https://doi.org/10.1021/cr970080y))
- 2 Prum, R. O. 2006 The anatomy, physics and evolution of avian structural color. In *Bird coloration, volume 1: mechanisms and measurements* (eds G. E. Hill & K. J. McGraw), pp. 295–353. Cambridge, MA: Harvard University Press.
- 3 Dufresne, E. R., Noh, H., Saranathan, V., Mochrie, S. G. J., Cao, H. & Prum, R. O. 2009 Self-assembly of amorphous biophotonic nanostructures by phase separation. *Soft Matter* **5**, 1792–1795. ([doi:10.1039/b902775k](https://doi.org/10.1039/b902775k))
- 4 Clarke, J. A., Ksepka, D. T., Salas-Gismondi, R., Altamirano, A. J., Shawkey, M. D., D'Alba, L., Vinther, J., DeVries, T. J. & Baby, P. 2010 Fossil evidence for evolution of the shape and color of penguin feathers. *Science* **330**, 954–957. ([doi:10.1126/science.1193604](https://doi.org/10.1126/science.1193604))
- 5 Suhonen, H., Fernandez, M., Serimaa, R. & Suortti, P. 2005 Simulation of small-angle x-ray scattering from collagen fibrils and comparison with experimental patterns. *Phys. Med. Biol.* **50**, 5401–5416. ([doi:10.1088/0031-9155/50/22/012](https://doi.org/10.1088/0031-9155/50/22/012))
- 6 Garnett, J. C. M. 1904 Colours in metal glasses and in metallic films. *Phil. Trans. R. Soc. Lond. A* **203**, 385–420. ([doi:10.1098/rsta.1904.0024](https://doi.org/10.1098/rsta.1904.0024))
- 7 Prum, R. O. & Torres, R. H. 2003 A Fourier tool for the analysis of coherent light scattering by bio-optical nanostructures. *Integr. Comp. Biol.* **43**, 591–602. ([doi:10.1093/icb/43.4.591](https://doi.org/10.1093/icb/43.4.591))
- 8 Prum, R. O. & Torres, R. 2003 Structural colouration of avian skin: convergent evolution of coherently scattering dermal collagen arrays. *J. Exp. Biol.* **206**, 2409–2429. ([doi:10.1242/jeb.00431](https://doi.org/10.1242/jeb.00431))
- 9 Prum, R. O., Dufresne, E. R., Quinn, T. & Waters, K. 2009 Development of colour-producing β -keratin nanostructures in avian feather barbs. *J. R. Soc. Interface* **6**, S253–S265. ([doi:10.1098/rsif.20080466.focus](https://doi.org/10.1098/rsif.20080466.focus))
- 10 Lingham-Soliar, T., Bonser, R. H. C. & Wesley-Smith, J. 2010 Selective biodegradation of keratin matrix in feather rachis reveals classic bioengineering. *Proc. R. Soc. B* **277**, 1161–1168. ([doi:10.1098/rspb.2009.1980](https://doi.org/10.1098/rspb.2009.1980))
- 11 Jones, R. A. L. 2002 *Soft condensed matter*. Oxford, UK: Oxford University Press.
- 12 Aissou, K., Kogelschatz, M. & Baron, T. 2009 Self-assembling study of a cylinder-forming block copolymer via a nucleation-growth mechanism. *Nanotechnology* **20**, ([doi:10.1088/0957-4484/20/9/095602](https://doi.org/10.1088/0957-4484/20/9/095602))